

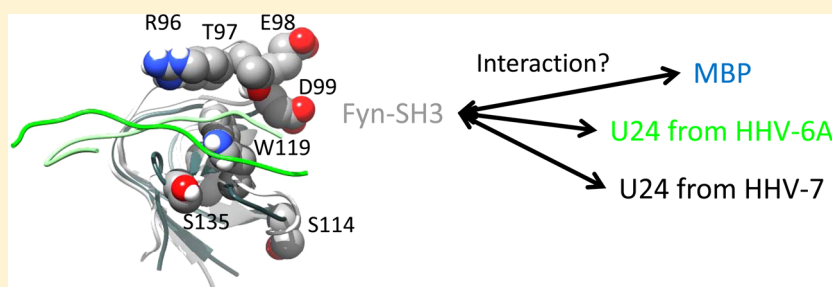
Probing the Interaction between U24 and the SH3 Domain of Fyn Tyrosine Kinase

Yurou Sang,[†] Andrew R. Tait,[†] Walter R. P. Scott,[†] A. Louise Creagh,[‡] Prashant Kumar,[†] Charles A. Haynes,[‡] and Suzana K. Straus^{*,†}

[†]Department of Chemistry, University of British Columbia, 2036 Main Mall, Vancouver, BC V6T 1Z1, Canada

[‡]Michael Smith Laboratories, University of British Columbia, 2185 East Mall, Vancouver, BC V6T 1Z4, Canada

S Supporting Information



ABSTRACT: The putative membrane protein U24 from HHV-6A shares a seven-residue sequence identity (which includes a PxxP motif) with myelin basic protein (MBP), a protein responsible for the compaction of the myelin sheath in the central nervous system. U24 from HHV-6A also shares a PPxY motif with U24 from the related virus HHV-7, allowing them both to block early endosomal recycling. Recently, MBP has been shown to have protein–protein interactions with a range of proteins, including proteins containing SH3 domains. Given that this interaction is mediated by the proline-rich segment in MBP, and that similar proline-rich segments are found in U24, we investigate here whether U24 also interacts with SH3 domain-containing proteins and what the nature of that interaction might be. The implications of a U24–Fyn tyrosine kinase SH3 domain interaction are discussed in terms of the hypothesis that U24 may function like MBP through molecular mimicry, potentially contributing to the disease state of multiple sclerosis or other demyelinating disorders.

A number of studies have shown that both human herpes virus type 6 (HHV-6)^{1,2} and type 7 (HHV-7)^{3,4} have been implicated in multiple sclerosis (MS), though some evidence suggests that MS is not necessarily the result of active herpes virus infection.⁵ Both of these viruses have the putative membrane protein U24 in common, which contains a proline-rich region (Figure 1). The proline-rich segment of U24 from HHV-6A is identical to that found in myelin basic protein (MBP) (Figure 1). Evidence has shown that T-cells from MS patients could be activated by a U24 peptide containing the PRTPPPS sequence and cross-react with MBP.¹ We have also demonstrated that, like MBP, U24 from HHV-6A can be phosphorylated at the threonine position within this segment.⁶ The threonine in the sequence is a MAP kinase phosphorylation site in MBP and may be important for myelin sheath membrane organization and compaction. MS patients have a degree of phosphorylation at this site lower than that of normal individuals. This shared sequence between U24 and MBP may also be important because it represents a PxxP recognition motif site that binds to the SH3 domain of Fyn tyrosine kinase,⁷ an interaction that is important for tethering the actin filaments of the cytoskeletal scaffolding to the cell membrane.⁸ As the organization of the cytoskeleton is important for the structural integrity of the myelin sheath, it is quite possible that

U24 may act to destabilize the myelin sheath membrane by blocking MBP's interaction with Fyn tyrosine kinase, again by way of the identical sequence.

Fyn kinase has been shown to have a pivotal function in translating complex communication signals into different cellular responses to direct central nervous system (CNS) myelination.⁹ The essential functional involvement of Fyn in myelination was shown by using mutant mice lacking Fyn or expressing a single amino acid mutant kinase-inactive form of Fyn.^{10–12} Hypomyelination in these mice is found in different regions of the brain and optic nerve; the number of myelin fibers is drastically reduced. Blocking Fyn activity with selective inhibitors or with a dominant negative form of Fyn (lacking kinase activity) interferes with oligodendroglial maturation by slowing oligodendroglial process formation and outgrowth.^{12,13} The full cast of molecules with which Fyn functionally interacts is unknown, but Fyn is considered thus far to mediate downstream signaling of three major pathways: (i) the Rho family GTPases that in turn regulate actin cytoskeleton dynamics essential to cell survival and morphological differ-

Received: July 30, 2014

Revised: September 3, 2014

Published: September 7, 2014

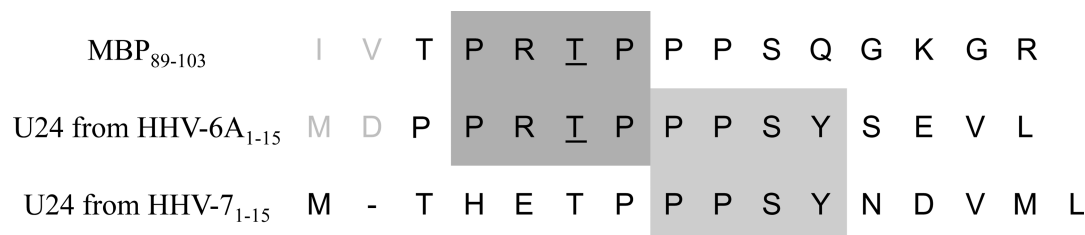


Figure 1. Sequences of MBP (residues 89–103, numbering used to correspond to numbering in the murine classic 18.5 kDa MBP isoform¹⁷), U24 from HHV-6A (residues 1–15), and U24 from HHV-7 (residues 1–15). The PxxP motif, which is common to MBP and U24 from HHV-6A, is highlighted in dark gray, while the PPxY motif, which is common to U24 from HHV-6A and HHV-7, is highlighted in light gray. The first residues of MBP and U24 from HHV-6A are colored gray to show that they were not included in the MD simulation.

entiation, (ii) recruitment of microtubule cytoskeleton component polarity to direct cargo transport, and (iii) control the transport, stability, and translation of mRNA of myelin proteins, especially MBP.⁹

Fyn kinase belongs to the Src family of nonreceptor tyrosine kinases and has a mass of 59 kDa. It has four Src homology (SH) domains:¹⁴ a SH4 domain at the N-terminus with two acylation sites to anchor Fyn to the cell membrane, SH3 and SH2 protein binding domains, and a SH1 domain with kinase activity. Recently, a number of elegant studies have demonstrated that MBP binds to Fyn-SH3 by adopting a polyproline PPII helix structure, causing Fyn-SH3 to bind to lipids.^{7,8,15–17} In particular, it was shown that it is specifically the PRTPPPS segment that contains the PxxP SH3 ligand motif that is critical for the interaction between MBP and Fyn-SH3.

It is conceivable that a foreign protein, such as one from a virus or bacterium, can bind to Fyn-SH3 and compete with essential interactions, such as Fyn–Tau association, thereby bringing about dysfunction in myelination. Hepatitis C-encoded NS5a protein has relatively high affinity for Fyn-SH3 ($K_D = 629$ nM) and could potentially compete with native host proteins for binding to Fyn-SH3.¹⁸ As discussed above, U24 protein from HHV-6 (6A and 6B) has the PRTPPPS sequence in common with MBP (Figure 1). Therefore, it is possible that U24 may bind to Fyn-SH3 to prevent it from interacting with its cytoskeleton-organizing partners such as Tau or MBP.

The goal of this study was to probe whether a specific interaction between U24 and Fyn-SH3 exists and to be able to further hypothesize how the interaction may relate to a dysfunction in myelination. In other words, a specific interaction between U24 and Fyn-SH3 via the PxxP motif would lend support to the U24/MBP mimicry hypothesis^{6,19} over alternative hypotheses such as the one that other motifs, e.g., PPxY, shared by both U24 proteins from HHV-6 and -7 (Figure 1) may play a role in modifying the integrity of the myelin sheath.^{3,20} To allow detection of interactions between U24 and Fyn-SH3, we utilized GST pull-downs, NMR spectroscopy, and isothermal titration calorimetry (ITC). Furthermore, circular dichroism was used to determine if the polyproline motif in U24 can adopt a PPII helix, as was found for MBP.⁷ Finally, molecular dynamics simulations were performed to compare the MBP–Fyn-SH3 interaction to the U24–Fyn-SH3 interaction at an atomic level. A number of constructs were tested: U24 from HHV-6A, NΔ9-U24 from HHV-6A (with the PRTPPPS segment removed), U24 from HHV-7, and two peptides representing the first 15 N-terminal

residues of U24 from HHV-6A (Figure 1) and HHV-7 (Figure 1).

MATERIALS AND METHODS

Expression of GST-Fyn-SH3. The plasmid expressing the GST-Fyn-SH3 protein was a kind gift from C. Pallen (Child & Family Research Institute, Vancouver, BC). The vector is pGEX-KG with the SH3 domain of human Fyn (from residues TGVTLF to YVAPVD) cloned into the HindIII–XbaI site. The protein expressed is Fyn-SH3 at the C-terminus of GST, with a thrombin cleavage site between them. Further details of the expression and purification of this construct can be found in the Supporting Information.

Construction, Expression, and Isolation of NΔ9-U24, a Deletion Mutant of U24 from HHV-6A with the Nine N-Terminal Amino Acids Removed. U24 lacking the nine amino acids at its N-terminus (MDPPRTPPP removed) was obtained by performing site-directed mutagenesis on a plasmid encoding wild-type U24, designated pMAL-p2x-U24,^{6,20} which expresses the U24 protein at the C-terminus of maltose binding protein by a hexahistidine tag. Instructions for the Quikchange II Site-Directed Mutagenesis Kit (Stratagene) were followed. Briefly, mutagenic primers were designed with the following sequences: 5′-catcatcacagcagcgccgtgtgcccgcggcagctactccgaagtctg-3′ (forward primer) and 5′-gtgcggggaacctgaccgcataacgtccatcatcagaactcggatgagctgcccgcg-3′ (reverse primer). After polymerase chain reaction (PCR) had been conducted, the parental plasmid was digested with 10 units of DpnI restriction endonuclease (Invitrogen) and the amplified mutagenic plasmid was used to transform XL1-Blue *Escherichia coli*. Transformed *E. coli* was plated on LB-agar plates containing 50 μg/mL carbenicillin and incubated overnight at 37 °C. Single colonies were selected for colony PCR using the primers pMAL-seq and pMAL-seqrv (5′-ggtcgctcagactgtcgatgaagcc-3′ and 5′-cgccagggtttccagtcacgac-3′, respectively). Amplified reactions were conducted via agarose gel electrophoresis, and bands that were smaller than wild-type control plasmid reactions were suggestive of successful mutagenesis in those colonies. These colonies were selected for growth in 5 mL of LB containing 50 μg/mL carbenicillin overnight at 37 °C, while being shaken at 225 rpm. Plasmids were isolated using QIAprep Spin Miniprep Kits (Qiagen) and sent for sequencing at the NAPS Unit of the University of British Columbia.

Purification was conducted in the same fashion as previously reported for wild-type U24.^{6,20} The mass of the isolated mutant NΔ9-U24 protein was obtained by matrix-assisted laser desorption ionization time-of-flight (MALDI-TOF) mass spectrometry, which confirmed that the protein had the desired mutation, having an N-terminal sequence of nine amino acids

(MDPPRTPPP) truncated and beginning with the sequence GSYSEVL.

Construction, Expression, and Purification of U24 from HHV-7. The full-length gene of U24 from HHV-7 was obtained by overlap PCR, using the primers and oligonucleotide fragments (IDT) listed in Table S1 of the Supporting Information. The N-terminus of the sequence was fused to a hexahistidine tag and a tobacco etch virus (TEV) protease cleavage site and then cloned into pMAL-c2x using BamHI–HindIII sites. The construct was expressed in Origami 2 (Novagen) *E. coli* at 37 °C in LB and induced using 0.3 mM IPTG. The cells continued to grow for 4 h, after which they were harvested by centrifugation. The cells were lysed in 30 mL of lysis buffer [20 mM KH₂PO₄, 0.5 M NaCl, 1% Triton X-100, and 10 mM imidazole (pH 7.4)] by three passes through a French press (Aminco). The lysate was stirred for 2 h with 6 M urea at 4 °C and then centrifuged at 25000g and 4 °C for 1 h. The supernatant was loaded onto a column containing 5 mL of Ni-NTA agarose (Qiagen) and washed with 75 mL of lysis buffer and 25 mL of washing buffer [20 mM KH₂PO₄, 0.5 M NaCl, 1% Triton X-100, and 25 mM imidazole (pH 7.4)]. The construct was eluted using 25 mL of elution buffer [20 mM KH₂PO₄, 0.5 M NaCl, 1% Triton X-100, and 500 mM imidazole (pH 7.4)]. The elution fraction was dialyzed against Tris buffer [50 mM Tris and 0.5% Triton X-100 (pH 7.8)] with a 2000 MWCO dialysis membrane (Spectrum Laboratories). The dialyzed fraction was transferred to a falcon tube and supplemented with 1 mM DTT. The digestion mixture was inverted end over end with 0.2 mg of TEV protease (made in house) at 4 °C for 16 h. The cleaved U24 from HHV-7 was purified by being passed through the Ni-NTA column again, and the residual MBP was trapped on a Q-Sepharose column (GE Healthcare). The flow-through fraction was dialyzed against pull-down buffer (*vide infra*).

GST-Fyn-SH3 Pull-Down Assays with Full-Length U24 from HHV-6A, Mutant NΔ9-U24 from HHV-6A, and Full-Length U24 from HHV-7. In separate microcentrifuge tubes, 30 μL of Glutathione-Sepharose 4B beads (GE Healthcare) was added and equilibrated by adding 1 mL of pull-down buffer containing 20 mM potassium phosphate, 75 mM NaCl, and 0.5% Triton X-100 (pH 7.4) via centrifugation at 2000 rpm in a microcentrifuge (Fisher Scientific) for 5 min at 4 °C. The buffer was removed, and 1 mL of fresh buffer was added and centrifuged again. This procedure was repeated a third time. To the equilibrated beads was added 30 μL of GST or GST-Fyn-SH3. GST and GST-Fyn-SH3 stocks were dialyzed with pull-down buffer overnight, and the concentrations were determined by a BCA assay to be 1.52 and 1.22 mg/mL, respectively. Pull-down buffer was added to a final volume of 500 μL with the bead slurry. Afterward, the beads were pelleted by centrifugation and rinsed three times with 0.5 mL of pull-down buffer with intermittent centrifugation and replacement with fresh buffer. A stock solution of either version of U24 or NΔ9 (0.15 mg/mL protein in pull-down buffer for U24 and NΔ9 from HHV-6A; 0.10 mg/mL for U24 from HHV-7) was added in a volume of 500 μL (750 μL for U24 from HHV-7) to the beads, and the slurry was mixed again with end-over-end rotation for 30 min at 4 °C. The beads were pelleted by centrifugation, and the supernatant was removed. The beads were washed with three successive rounds of 0.5 mL of Glasgow Lysis Buffer (GLB),²¹ which consists of 10 mM PIPES-NaOH, 120 mM KCl, 30 mM NaCl, 5 mM MgCl₂, 1% Triton X-100, and 10% glycerol, with centrifugation and removal of the supernatant

before each addition of fresh buffer. The beads were then mixed with 30 μL of 2× Novex dye (Invitrogen) supplemented with 5% β-mercaptoethanol, vortexed briefly, and then heated for 5 min at 95 °C. A volume of 25 μL was removed and subjected to sodium dodecyl sulfate–polyacrylamide gel electrophoresis (SDS–PAGE) using a Tris-Tricine buffer system, and then the gel was stained with Coomassie G-250. For U24 from HHV-7, 10 μL was removed for electrophoresis and stained with silver stain.

Construction of a 15-Residue Peptide Representing the Polyproline-Containing N-Terminus of U24 from HHV-6A and HHV-7. Two synthetic 15-mer peptides representing the N-terminus of U24 from HHV-6A and HHV-7 (Figure 1) were obtained using standard solid-phase peptide synthesis protocols,^{22,23} employing 9H-fluoren-9-ylmethoxycarbonyl (Fmoc)-based *N*-α-amino acid group protection. Double coupling was required for the last nine residues (MDPPRTPPP) of the peptide representing the N-terminus of U24 from HHV-6A. For the peptide based on the N-terminal sequence of U24 from HHV-7, eight residues (MTHETPPP) were double coupled. In both cases, the synthetic peptide was purified by preparative gradient RP-HPLC on a Waters 600 system with a Waters 2996 photodiode array detector with 229 nm UV detection using a Phenomenex C4 or C18 column (20 μm, 2.1 cm × 25 cm) at a flow rate of 10 mL/min, with a gradient of 0 to 35% buffer B (10% deionized water and 90% acetonitrile containing 0.1% TFA) in buffer A (90% deionized water and 10% acetonitrile containing 0.1% TFA) over 40 min. The peptide solution was lyophilized, and its final mass was confirmed by MALDI-TOF mass spectrometry (for U24 from HHV-6A, experimental mass of 1685.8 Da and theoretical mass of 1685.9 Da; for U24 from HHV-7, experimental mass of 1731.6 Da and theoretical mass of 1731.96 Da).

Isothermal Titration Calorimetry. Unlabeled Fyn-SH3 was expressed and purified as described above. The cleaved SH3 domain was dialyzed with 40 mM sodium phosphate buffer (pH 6.0) overnight and then concentrated using a 4 mL Amicon ultracentrifugal filter device with a MWCO of 3000 Da (Millipore). The final protein concentration was determined by the BCA protein assay to be 1.10–1.48 mM, and the pH was 6.09. A 20× peptide solution was made by dissolving purified and lyophilized U24 from HHV-6A peptide in the same buffer (final concentration of 27.6 mM). The pH was checked with a micro pH meter (Thermo Scientific) and adjusted to match that of the protein solution. The protein sample was filtered using a 0.22 μm filter (Millipore). The peptide solution was placed in an Eppendorf tube (1.5 mL) and centrifuged on a tabletop microcentrifuge (Fisher Scientific) at 13000 rpm for 20 min at 4 °C. The supernatant was transferred to a new tube. Both protein and peptide were degassed at 25 °C for 4–8 min before being loaded into the sample chamber and syringe, respectively.

Isothermal titration calorimetry experiments were performed using an iTC200 microcalorimeter (GE Healthcare) at 25 °C. The titration protocol comprised of a preliminary injection of 0.4 μL of the peptide solution, followed by 19 consecutive 2 μL injections into the sample cell (200 μL) containing Fyn-SH3. The time between each injection was 150 s. Control titrations of the peptide sample into protein-free buffer, as well as buffer into the Fyn-SH3 sample (to verify the lack of protein oligomerization effects), were also conducted. The heats of dilution for the peptide were subtracted from the original heats

prior to data fitting to a bimolecular interaction model to obtain K_a (association constant, in inverse molar) and ΔH (enthalpy of binding, in kilocalories per mole) at a binding stoichiometry n (number of binding sites per Fyn-SH3) of 1.0. The ITC experiment was repeated three times with mean values and standard deviations reported.

^1H – ^{15}N HSQC NMR Titrations and K_D Calculations for the Fyn-SH3 Protein and U24 Peptide Interaction. Solutions of [^{15}N]Fyn-SH3 were prepared by successive rounds of concentration and dilution with NMR buffer²⁴ [10 mM sodium phosphate, 10% D_2O , 0.5 mM benzamidine, and 0.1% sodium azide (pH 6.0)] using a 15 mL regenerated cellulose centrifugal filter device with a MWCO of 3000 Da (Millipore). The final protein concentration was determined using an extinction coefficient (ϵ_{280}) of $16960\text{ cm}^{-1}\text{ M}^{-1}$, calculated using the method of Edelhoch²⁵ but with the extinction coefficients of Trp and Tyr determined by Pace,²⁶ as used by the protparam algorithm at <http://www.expasy.ch>. The concentration was also verified by using the BCA protein assay (Pierce) and found to be 0.4–0.6 mM. Protein solutions were centrifuged briefly and diluted to a final volume of 500 μL with NMR buffer. These were placed in a 5 mm NMR tube, and a ^1H – ^{15}N HSQC spectrum was recorded at 25 $^\circ\text{C}$ using a Bruker (Milton, ON) 850 MHz NMR spectrometer, using a cryoprobe (for the peptide from HHV-7, the spectra were recorded on a Bruker 500 MHz instrument at 30 $^\circ\text{C}$). Peptide binding was analyzed by adding small volumes of unlabeled U24 peptide [from HHV-6A and HHV-7 (Figure 1)] stock solution that had a concentration of 29.25 mM for the U24 peptide from HHV-6A and 38.5 mM for the U24 peptide from HHV-7 in NMR buffer. HSQC spectra were recorded after each subsequent addition. A total of 14–15 different protein:peptide ratios between 1:0 and 1:12.6 for U24 from HHV-6A and 1:13.5 for U24 from HHV-7 were examined. The pH of the solution was measured to be 6.3 at the start of the titration and found to be identical after the last addition of peptide. The amide chemical shifts of Fyn-SH3 were assigned using previously published assignments by Mal et al.²⁷ and verified using a three-dimensional (3D) HSQC-NOESY data set obtained on an 850 MHz spectrometer. The dissociation constant (K_D) was calculated according to the method described by Zarrine-Afsar et al.²⁸ The chemical shift at a peptide concentration C is defined as

$$\Omega(C) = \Omega_0 + f_B(\Omega_f - \Omega_0) + mC$$

where $\Omega_0 = \Omega(0)$, $\Omega_f = \Omega(\infty)$, and m is a baseline correction factor.²⁸ In this case, the fraction of Fyn-SH3 bound to the peptide is related to K_D :²⁸

$$f_B = \frac{C}{C + K_D}$$

Parameters m and K_D are allowed to vary to optimize the fit between the experimental and calculated chemical shift values.

^1H – ^{15}N HSQC NMR Spectra of [^{15}N]Fyn-SH3 with Full-Length U24 and ΔN9 -U24 from HHV-6A. Full-length U24 or ΔN9 -U24 from HHV-6A was prepared from an acetone precipitate procedure, as previously described.¹⁹ Dodecylphosphocholine (DPC) (Avanti Polar Lipids) in chloroform was placed in a 5 mL round-bottom flask and dried to a thin film under nitrogen. Enough DPC was added so that a final concentration of 6 mM in 500 μL could be obtained. Residual chloroform was removed overnight under vacuum. A volume of

500 μL of 20 mM MES (pH 6.2) was used to reconstitute the lipid solution, and the resulting solution was used to dissolve full-length U24 or ΔN9 -U24 with extensive sonication in a water bath. The dissolved protein was transferred to a Vivaspinn 500 (GE Healthcare) centrifugal filtration unit with a MWCO of 3000 and buffer exchanged into NMR buffer according to the manufacturer's protocols. After several rounds of concentration and redilution into NMR buffer, U24 or ΔN9 -U24 was reconstituted to a final concentration of 0.15 mM together with 0.25 mM [^{15}N]Fyn-SH3, 7% D_2O , and NMR buffer to a final volume of 500 μL . Given the critical micelle concentration of DPC and its aggregation number, this sample represents a U24:DPC ratio of one U24 molecule per DPC micelle. The U24:Fyn ratio is 1:0.6. These solutions were placed in a 5 mm NMR tube, and ^1H – ^{15}N HSQC spectra were recorded at 30 $^\circ\text{C}$ using a Bruker 500 MHz NMR spectrometer.

Circular Dichroism of N-Terminal Peptide U24 from HHV-6A. CD experiments were conducted on a Jasco J-815 instrument equipped with a circulating temperature-controlled water bath. The synthetic U24 peptide was dissolved in 10 mM sodium phosphate and 10 mM KCl (pH 6.5) to a final concentration of 0.3 mg/mL. A volume of 300 μL of peptide solution was placed in a cuvette with a path length of 0.1 cm. Scans were collected at a rate of 100 nm/min in 0.1 nm intervals, in the 190–250 nm wavelength range. Starting at 5 $^\circ\text{C}$, we collected scans at 5 $^\circ\text{C}$ increments to 65 $^\circ\text{C}$. A total of four scans were collected at each temperature and averaged. Buffer blank spectra were similarly collected at each temperature and then subtracted from the corresponding peptide spectra. The raw data in millidegrees were converted to mean residue ellipticity. To characterize the PPII helical content, the spectrum at 45 $^\circ\text{C}$ was subtracted from that taken at 5 $^\circ\text{C}$.⁷

Molecular Dynamics Simulations. Three simulations were set up using the starting structure deposited in the Protein Data Bank (PDB) (entry 1A0N, model 1²⁹). The simulations were run on 1A0N (PI3 kinase peptide) for comparison with an experimental structural model. In the other two simulations, the coordinates of the MBP and U24 peptides investigated (Figure 1) were generated by using the “swapa” functionality in UCSF CHIMERA.^{30,31} The GROMOS96^{32,33} biomolecular simulation package and the 43A1 force field³² were used. The models were solvated in explicit SPC water.³⁴ Rectangular periodic boundary conditions were imposed. Simulations were performed in the NPT ensemble ($T = 300\text{ K}$, and $P = 1\text{ atm}$) using the Berendsen weak coupling methods.³⁵ Covalent bonds were constrained using the SHAKE method,³⁶ with a relative geometric tolerance of 10^{-4} . A reaction field³⁷ long-range correction to the truncated Coulomb potential was applied. Each of the simulations was run for 20 ns, after equilibration for 1 ns.

RESULTS

Pull-Down Experiments with GST-Fyn-SH3 and U24 from HHV-6A and HHV-7. To determine if U24 interacts with Fyn-SH3 via the PxxP motif in U24 that is common with MBP, a pull-down experiment was performed using GST-Fyn-SH3 and full-length U24 from HHV-6A. A similar pull-down experiment was performed using full-length U24 from HHV-7, which does not have the canonical PxxP motif, but rather a PPxY motif in common with U24 from HHV-6A. Peptides devoid of the PxxP motif have recently been shown to nevertheless bind SH3 domains.^{38,39} Therefore, if all controls

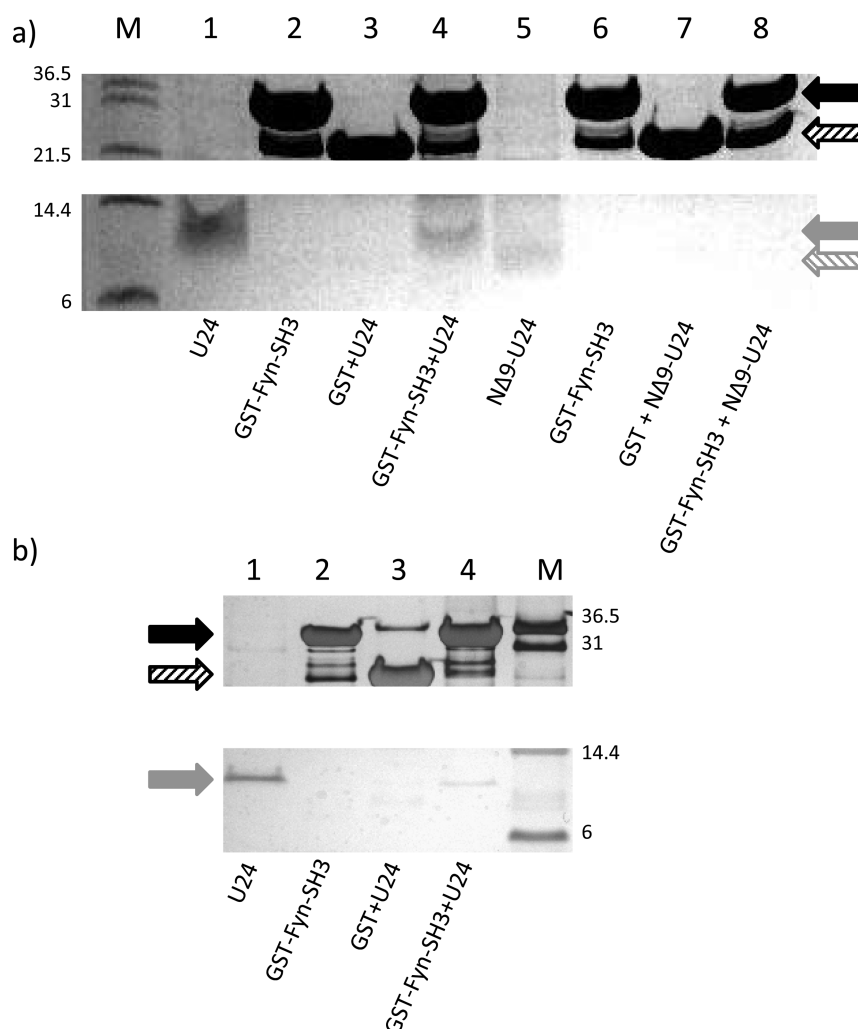


Figure 2. SDS–PAGE results of a GST pull-down experiment with Fyn-SH3 and U24: (a) U24 (solid gray arrow) and NΔ9-U24 (dashed gray arrow) from HHV-6A and (b) U24 from HHV-7 (solid gray arrow). In panel a, U24 and NΔ9-U24 were loaded as references in lanes 1 and 5, respectively. U24 appears to bind to Fyn-SH3 via its PxxP domain (lane 4), but truncated NΔ9-U24 without the PxxP motif cannot bind Fyn-SH3 (lane 8). The gel was stained with Coomassie Blue G-250. In panel b, U24 is loaded as a reference in lane 1. U24 from HHV-7 appears to bind only very weakly to Fyn-SH3, as seen from the very faint band in lane 4. In panel b, the gel is stained with silver stain. The marker lanes and corresponding molecular weights are indicated by lane M in panels a and b. The tops of the gels in panels a and b show the GST-Fyn-SH3 (solid black arrow) and GST (dashed black arrow) bands. The presence of two bands where GST-Fyn-SH3 was loaded indicated that the sample consisted mainly of GST-Fyn-SH3, with a minor contribution from GST alone. Because GST alone and U24 do not interact (lane 3 in panels a and b), the presence of this minor impurity does not affect the outcome of the pull-down experiment.

were included, GST-Fyn-SH3, GST, U24 (from HHV-6A and HHV-7), and NΔ9-U24 (from HHV-6A only) were purified.

Figure 2a depicts a SDS–PAGE gel demonstrating that full-length U24 from HHV-6A could interact with GST-Fyn-SH3 that was bound to glutathione beads (lane 4) but U24 did not interact with GST alone (lane 3). This result indicates that U24 from HHV-6A can bind to the SH3 domain of Fyn. To see if this interaction was mediated specifically by the polyproline region of U24 from HHV-6A, the NΔ9-U24 mutant, which lacks the nine N-terminal amino acids (containing the PxxP SH3 recognition site), was mixed with GST-Fyn-SH3, and no interaction was observed (lane 7). Control U24 (lane 1) and NΔ9-U24 (lane 5) proteins were loaded for reference. For U24 from HHV-7, the interaction with Fyn-SH3 is clearly much weaker, as seen from the very faint band detected with silver stain in lane 4 (Figure 2b).

These results, taken together, suggest that U24 from HHV-6A preferentially binds to Fyn-SH3 via its PxxP motif. In the

absence of this motif, such as in the deletion mutant or in U24 from HHV-7 (with the PPxY motif), little to no interaction is observed. The pull-down results, loaded with nearly all U24 bound by 30 μ L of resin, also suggest that the binding interaction is possibly not a strong one.

ITC Experiments. To ascertain the strength of the binding interaction between U24 and Fyn-SH3, ITC experiments were conducted. Because the pull-down results suggest that the strongest interaction is between U24 from HHV-6A, this pair was investigated in detail. The mean thermodynamic parameters averaged from three independent experiments are listed in Table 1, with a characteristic ITC experiment and associated heat of dilution run shown in Figure 3. Control experiments with buffer in a Fyn-SH3 solution showed no evidence of protein aggregation or dissociation. Much weaker binding was observed by ITC for titrations of U24 HHV-7 into Fyn-SH3 ($K_D \approx 8$ –10 mM).

Table 1. Parameters for U24 from HHV-6A Binding to Fyn-SH3 at 25 °C^a

	K_D (mM)	ΔG (kJ mol ⁻¹)	ΔH (kJ mol ⁻¹)	ΔS (J mol ⁻¹ K ⁻¹)
ITC ^b	5.1 ± 0.3	-13.1 ± 0.2	-12.5 ± 0.6	2 ± 2
NMR ^c	5 ± 1			

^aThe stoichiometry, n , was fixed at 1.0 while fitting the ITC data. ^bThe data were obtained from an average of three runs. The errors represent the standard deviation. ^cThe binding constant was determined by averaging the K_D value determined for four of the perturbed residues: R96, T97, W119s, and I133.

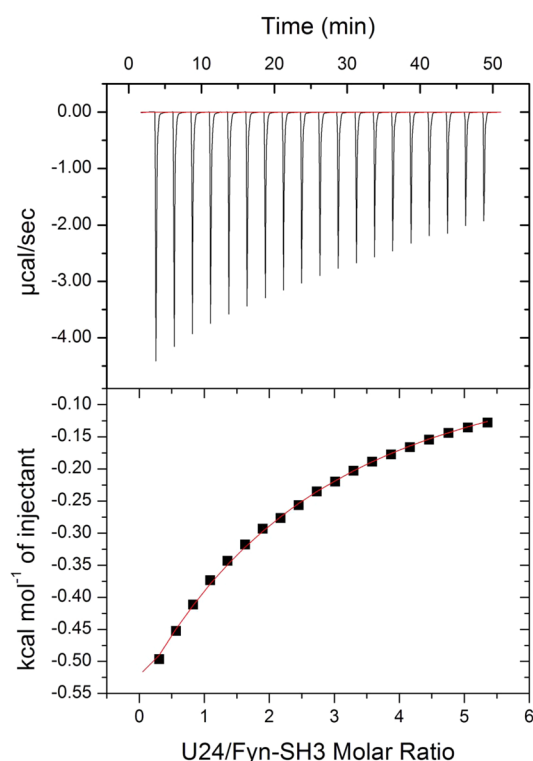


Figure 3. ITC data for U24 from the HHV-6 peptide (U24 from HHV-6A₁₋₁₅) binding to Fyn-SH3 at 25 °C. The other two runs produced data that looked nearly identical. The top panel shows raw titration data for 2 μ L injections of 27.6 mM U24 peptide into the ITC cell containing 1.48 mM Fyn-SH3 in 40 mM sodium phosphate (pH 6.0). The bottom panel shows integrated heat data (■) and a best fit (—) to a one-site binding model.

Titration of U24 Peptides by NMR. As ITC demonstrates that the interaction between U24 and Fyn-SH3 is weak, ¹H-¹⁵N HSQC NMR spectroscopy was performed, using ¹⁵N-labeled Fyn-SH3 and titrating in increasing amounts of U24 peptides representing the 15 residues at the N-terminus of U24 from HHV-6A (Figure 4a and Figure S1a of the Supporting Information) and HHV-7 (Figure 4b and Figure S1b of the Supporting Information). Several amide chemical shifts of Fyn-SH3 changed in response to the addition of U24₁₋₁₅ from HHV-6A (Figure 4a) and continued to change until a sufficiently high peptide:protein ratio was reached, indicative of binding saturation. The most notable shift changes were for residues Arg96 and Thr97 (Figure S1a of the Supporting Information), which are known to be part of the RT loop,⁴⁰ a flexible region of SH3 domains that is critical for peptide selectivity and binding. These residues were also perturbed in the case of titration with U24₁₋₁₅ from HHV-7 (Figure S1b of

the Supporting Information), but to a significantly lesser extent, further suggesting that U24 from HHV-7 interacts more weakly and nonspecifically with Fyn-SH3 than its HHV-6A counterpart. Indeed, the chemical shift perturbations for U24 from HHV-7 are smaller than those found for U24 from HHV-6A. In addition, the perturbations are not limited to specific residues, suggesting that a specific binding site does not exist for U24 from HHV-7 and Fyn-SH3 (Figure S1 of the Supporting Information).

Little line broadening was observed during the titration, indicating that exchange between the bound and unbound states is fast on the NMR time scale. Under these conditions, the shift in peak position relative to the spectrum of Fyn-SH3 alone is directly proportional to the fraction of the bound state, assuming two-state binding. Fitting the binding data for U24 from the HHV-6A peptide using the method by Zarrine-Afsar et al.²⁸ yielded a binding constant of 5 ± 1 mM (Table 1), using a number of perturbed amide resonances. This is in agreement with the values determined via ITC (Table 1). The fraction of peptide bound, a parameter obtained during the K_D determination,²⁸ is plotted for a few representative residues in Figure 4c for U24 from HHV-6A. A binding constant (K_D) was estimated for U24 from HHV-7 and found to be ≈8–10 mM, in agreement with the results of ITC.

Interaction of Full-Length U24 and Truncation Mutant NΔ9-U24 with ¹⁵N-Labeled Fyn by NMR. To ensure that the binding observed as described above is relevant for full-length U24, ¹H-¹⁵N HSQC NMR experiments were also performed on ¹⁵N-labeled Fyn-SH3 in the presence of full-length U24 and truncation mutant NΔ9-U24. Because U24 from HHV-7 does not appear to interact strongly with Fyn-SH3, we focused here only on constructs from HHV-6A. Both U24 and the truncation mutant were solubilized in 6 mM DPC, as described in Materials and Methods, and added to a solution of ¹⁵N-labeled Fyn-SH3. Figure 5 shows the overlaid ¹H-¹⁵N HSQC spectra of Fyn-SH3 alone, Fyn-SH3 with full-length U24, and Fyn-SH3 with NΔ9-U24. Indicative of binding, only full-length U24 is able to perturb resonances in Fyn-SH3, while the spectrum acquired in the presence of NΔ9-U24 is virtually identical to the control spectrum that has no additional protein added to Fyn-SH3. In addition, the resonances that shift are those of residues similar to those shown in Figure 4, indicating that the binding interaction is located in a similar region of Fyn-SH3. This result further confirms that the full-length form of U24 is able to interact with Fyn-SH3 and that the PxxP motif is specifically required for this interaction.

Samples with higher DPC concentrations (required to solubilize more U24) were also prepared, but it was found that at higher DPC concentrations, the Fyn-SH3 resonances were perturbed, even in the absence of U24. This therefore precluded a full titration of Fyn-SH3 with full-length U24.

Far-UV CD of the U24 Peptide. Using the method described by Polverini et al.⁷ in their study of the polyproline region of MBP, the peptide representing the N-terminal region of U24 from HHV-6A was similarly investigated by temperature-variable circular dichroism (CD) spectroscopy. The presence of PPII helices is not readily apparent from the shape of far-UV CD spectra, which appear to be very similar to the spectra for a random coil peptide (Figure 6a). However, it was recently shown by Polverini et al. that close examination of CD spectra of PPII helix-containing peptides can reveal spectral subtleties attributed to the left-handed chirality of the PPII helix.^{41,42} Because of its extended structural conformation and

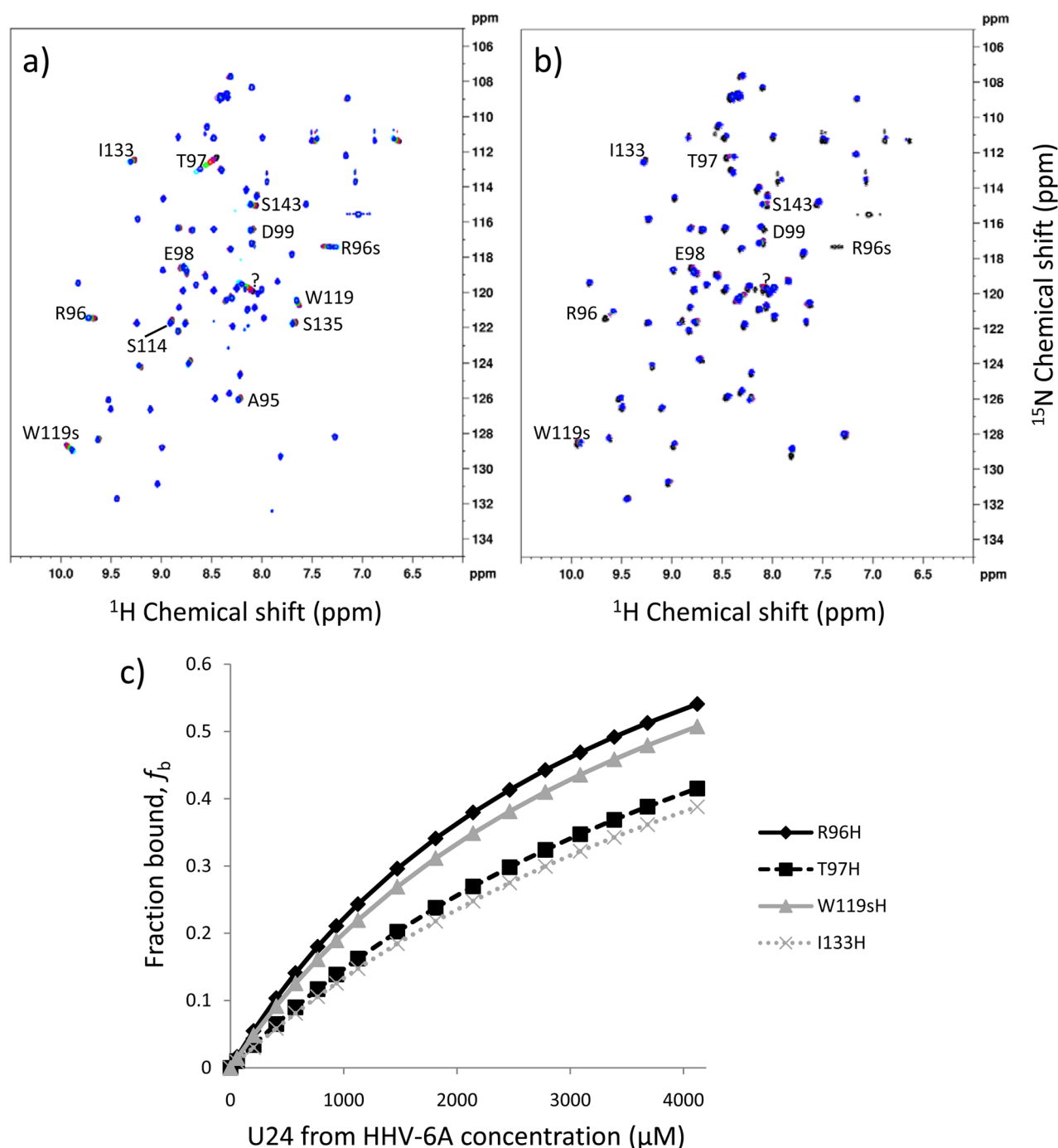


Figure 4. Overlay of ^{15}N - ^1H HSQC spectra of Fyn-SH3 with (a) the MDPPRTTPPSYSEVL peptide (U24 from HHV-6A₁₋₁₅) added in different Fyn-SH3:peptide ratios: of 1:0 (black), 1:1.08 (purple), 1:2.55 (red), 1:5.10 (green), 1:9.12 (blue), and 1:12.68 (cyan). Some of the key residues affected are indicated. The assignment is based on that reported by Mal et al.²⁷ and verified using 3D HSQC-NOESY. Side chains are denoted with the letter s. (b) Peptide MTHETPPPSYNDVML (U24 from HHV-7₁₋₁₅) added in different Fyn-SH3:peptide ratios: 1:0 (black), 1:0.98 (purple), 1:3.10 (red), 1:5.00 (green), and 1:8.30 (blue). The key residues affected are again indicated. The fit of the chemical shift data from panel a yielded the fraction of U24 from HHV-6A bound as a function of peptide concentration for select residues (using the method of Zarrine-Afsar et al.;²⁸ see the text for details): R96 (black, solid), T97 (black, dashed), W119s (gray, solid), and I133 (gray, dotted), as shown in panel c. The H at the end of each residue in the legend refers to the ^1H chemical shift. Similar calculations were performed on the basis of the ^{15}N chemical shift but are not shown. For further details about the chemical shift perturbations, see Figure S1 of the Supporting Information, which shows insets for R96 and T97 for U24 from HHV-6A₁₋₁₅ and U24 from HHV-7₁₋₁₅, as well as the normalized perturbations for all residues.

subsequent lack of NH \cdots O interresidue hydrogen bonding in the peptide backbone to stabilize the PPII helices, the helical structure is readily lost at higher temperatures. Difference spectra obtained by subtracting the spectrum acquired at 45 $^{\circ}\text{C}$ from that obtained at 5 $^{\circ}\text{C}$ are indicative of the PPII helix in the

U24 peptide (Figure 6b), which results in a maximum at ~ 220 nm and an isoelectronic point at ~ 210 nm (Figure 6a). These results are very similar to those obtained previously for the MBP peptide that contained the identical polyproline core sequence, PRTTPPS.⁷ U24, however, does appear to retain a

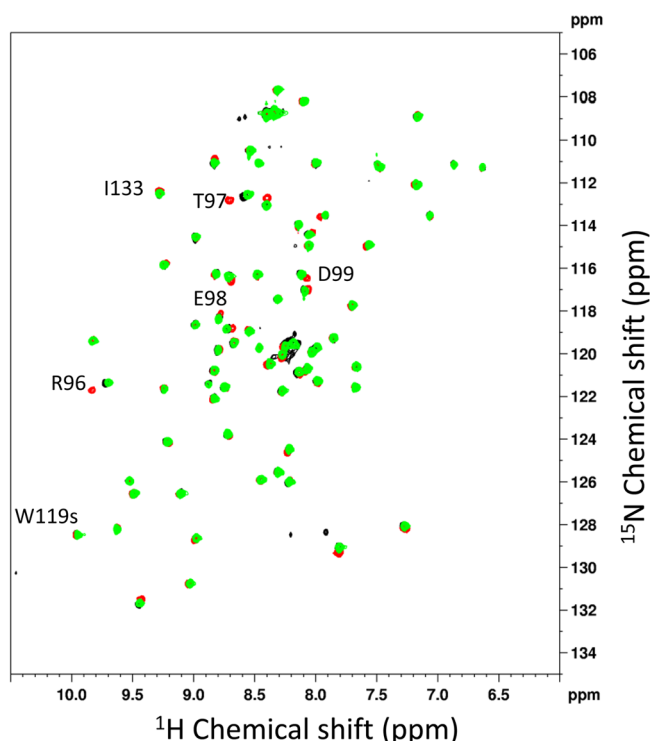


Figure 5. Overlay of ^{15}N – ^1H HSQC spectra of Fyn-SH3 alone (black), Fyn-SH3 in the presence of full-length U24 from HHV-6A (red), and Fyn-SH3 in the presence of NΔ9-U24 from HHV-6A (green) (i.e., U24 with the first nine residues removed). The samples consisted of 0.25 mM Fyn-SH3 in 6 mM DPC, 10 mM phosphate buffer (pH 6.0), and 7% D_2O . The U24 proteins were present in a ratio of 1:0.6 (Fyn-SH3:U24). The black and green spectra overlap almost completely.

significant amount of random coil signal even at 65 °C (CD minimum at ~202 nm), while the signal for the MBP peptide is virtually lost at this temperature. This may be due to the fact that the residues flanking the polyproline helix are different in U24 and MBP and therefore that they may engage in intermolecular interactions to further stabilize the PPII content at higher temperatures differently. This type of stabilization was proposed for full-length MBP, for which a similar trend in residual signal at higher temperatures was observed.

Molecular Dynamics Simulations of U24_{3–15} from HHV-6A and MBP_{91–103}. The starting structures after equilibration and final structures after 20 ns of the three simulated protein–peptide complexes are shown in Figure 7. The 1A0N peptide [light red starting structure, dark red final structure (Figure 7a)] hardly moves from the experimentally determined initial structure during the course of the simulation. The U24 peptide (light green starting structure, dark green final structure) adopts a slightly more elongated configuration, while maintaining contacts with many residues, shown in space-filling mode, observed to undergo chemical shift changes in the NMR experiments (Figure 7b). The largest conformational change of the three peptides is observed for MBP (light blue starting structure, dark blue final structure) (Figure 7c). In this final conformation, many additional hydrogen bonds are formed compared to the number in U24 (Figure 7d).

DISCUSSION

Fyn tyrosine kinase is localized mainly in the oligodendrocyte plasma membrane and plays an important role in a range of

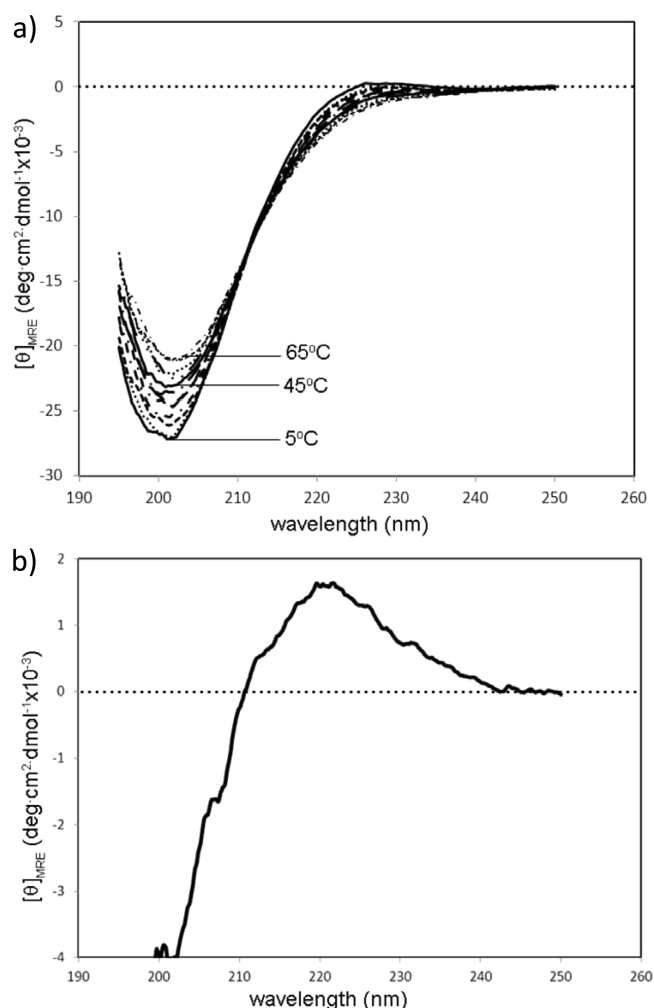


Figure 6. Variable-temperature far-UV CD of the 15-mer peptide containing the polyproline region U24 from HHV-6A (sequence of MDPPRTPPPSYSEVL). (a) CD spectra were collected from 190 to 250 nm at increasing temperatures, from 5 to 65 °C, in 5 °C. Subtracting the spectra at 45 °C from those obtained at 5 °C gives the difference spectra shown in panel b. The residual signal with a maximum at approximately 220 nm and an isochroic point at 210 nm is similar to results obtained for the polyproline-containing MBP peptide studied by Polverini et al.,⁷ indicative of the chiral nature of the left-handed polyproline helix that is transiently lost at higher temperatures.

signaling pathways via integrins and Ras activation during the development of the CNS.^{43,44} Fyn is particularly important in oligodendrocyte (OLG) differentiation and myelination.⁹ It has been demonstrated that the SH3 domain of Fyn interacts with myelin basic protein (MBP) via the PxxP binding motif in MBP.¹⁵ As a result of this interaction, an increase in the length of membrane processes and branching complexity in N19-OLG cultures was observed. It was therefore concluded that interactions of classic MBP isoforms with SH3 domain-containing proteins may play a physiological role in OLG differentiation and myelin formation, compaction, and overall stability.¹⁵ Furthermore, disruption of normal interactions between MBP and its intended SH3 domain partners in OLGs (i.e., Fyn) may lead to myelin dysfunction, leading to diseases like MS.

This study aimed to determine whether two similar but not identical forms of viral protein U24, from HHV-6A and HHV-

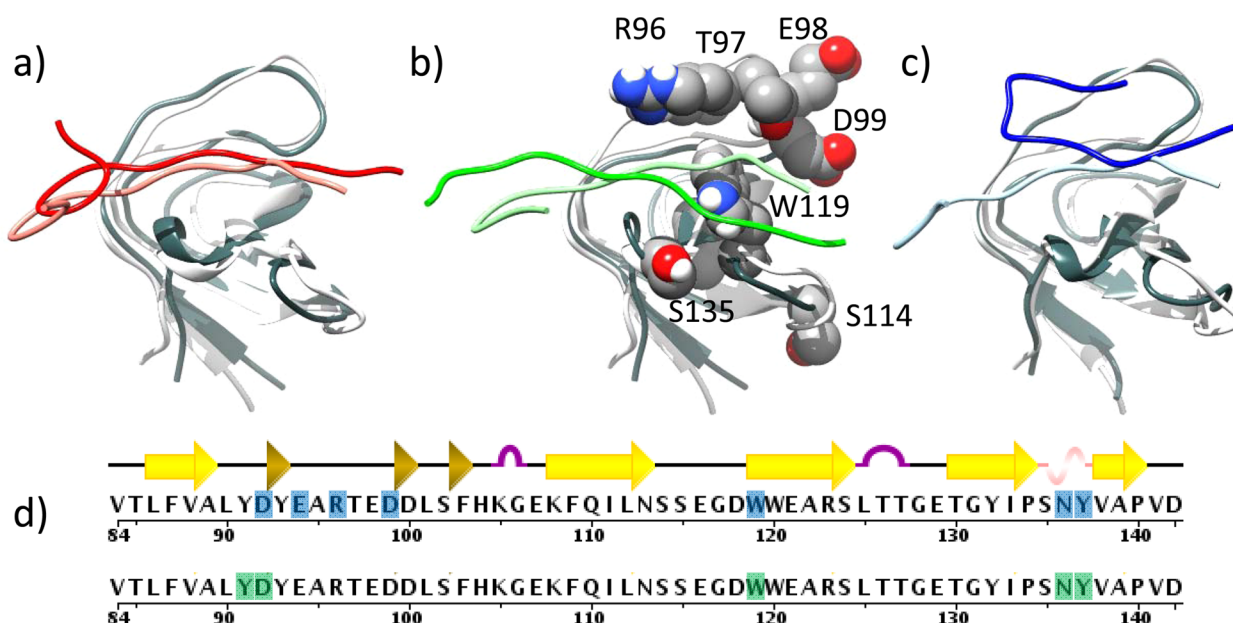


Figure 7. Starting and final structures of (a) 1A0N, (b) U24 from HHV-6A, and (c) MBP peptides (Figure 1). In each case, the model represented in the lighter colors is the starting structure whereas the model represented in the darker colors is the final structure, after simulation for 20 ns. In panel b, the residues that are perturbed in the NMR experiment are shown in CPK and some are labeled. In panel d is shown the primary sequence of Fyn-SH3, with the residues hydrogen bonding with MBP during the course of the simulation colored blue (above) and those interacting with the U24 peptide colored green (below). The sequence was obtained from PDB entry 1SHF, and the representation includes the secondary structure definitions as given in ref 47.

7, can potentially mimic binding of MBP to the SH3 domain of Fyn. U24 from HHV-6A shares an identical PxxP motif with MBP, whereas U24 from HHV-7 does not. However, both U24 proteins share a common PPxY motif. The data presented provide evidence that it is mainly the PxxP region in U24 from HHV-6A that interacts with the SH3 domain of Fyn tyrosine kinase. GST-tagged Fyn-SH3 can successfully bind to U24 HHV-6A via its PxxP region, and titrating a peptide of U24 containing this same region into Fyn-SH3 confirms a weak but specific interaction between the two partners [$K_D = 5$ mM (Table 1)]. When bound to a SH3 domain, U24 from HHV-6A fulfills the structural requirements for binding by forming a PPII helix (Figure 6), as also found for MBP.⁷ On the other hand, U24 from HHV-7 shows an even weaker interaction with Fyn-SH3. Evidence for this comes from the very weak band seen in the GST pull-down experiment (Figure 2b) and in the estimated K_D from NMR and ITC of approximately 8–10 mM. Overall, the data suggest that interaction with Fyn-SH3 occurs through a weak interaction with the PxxP motif of U24 from HHV-6A. This segment may be important and may explain why the binding interaction between the PI3 kinase peptide and Fyn-SH3 has a K_D of 16–50 μ M,²⁹ as this peptide has two PxxP motifs next to each other. Finally, the MD simulation data suggest that the residues surrounding the PxxP motif are also important, as more hydrogen bond contacts are observed in the MBP/SH3 simulation than in the U24-6A/SH3 counterpart (Figure 7d). Indeed, a shortened form of the U24 (from HHV-6A) peptide sequence missing the first two residues resulted in stronger binding between the 13-residue peptide and Fyn-SH3 [$K_D = 1$ –2 mM by NMR and ITC (data not shown)]. A number of studies on the importance of residues surrounding the PxxP motif for binding to Src homology 3 domains have been reported in the literature.^{18,24,45}

Previous work has shown that U24 from HHV-6A can be phosphorylated⁶ like MBP, and hence, it was suggested that

U24 from HHV-6A may be a mimic for MBP and be potentially involved in MS. The extent of phosphorylation of U24, however, is much weaker than that of MBP.⁶ Here we find that a binding interaction between U24 and Fyn-SH3 exists, but it is again most likely much weaker than the interaction between MBP and Fyn-SH3. Although a K_D value was never reported for MBP/Fyn-SH3, a crude estimate based on the data reported in ref 15 can be made ($K_D \approx 0.1$ –1 mM). This suggests that mimicry is possible but that perhaps explicit competition between U24 from HHV-6A and MBP in cells is less likely, unless *in vivo* conditions tip the balance in favor of U24. Some studies have suggested that weak protein–protein interactions may be a determinant of many biological processes.⁴⁶ It is also possible that U24 brings about myelin dysfunction by a completely different mechanism that could occur in conjunction to the mimicry of MBP or be entirely separate. For example, it is possible that the interaction of U24 with WW domains and the resulting cell surface downregulation of the transferrin receptor and other signaling and structural components affect myelin integrity.^{3,20} This hypothesis is currently being investigated.

■ ASSOCIATED CONTENT

Supporting Information

Expression protocols. This material is available free of charge via the Internet at <http://pubs.acs.org>.

■ AUTHOR INFORMATION

Corresponding Author

*E-mail: sstraus@chem.ubc.ca. Phone: (604) 822-2537. Fax: (604) 822-2847.

Funding

The research was supported by the Natural Sciences and Engineering Research Council of Canada.

Notes

The authors declare no competing financial interest.

ACKNOWLEDGMENTS

In addition to those already mentioned above, we are thankful for useful discussions with G. Harauz (Department of Molecular and Cell Biology, University of Guelph, Guelph, ON). We also thank the Canada Foundation for Innovation for funding the NMR spectrometers and the isothermal titration calorimeter used in this study.

ABBREVIATIONS

HHV-6A, human herpes virus type 6A; HHV-7, human herpes virus type 7; SH3, Src homology domain 3; MBP, myelin basic protein; NMR, nuclear magnetic resonance; HSQC, heteronuclear single-quantum coherence spectroscopy; MS, multiple sclerosis; DPC, dodecylphosphocholine; MWCO, molecular weight cutoff; ITC, isothermal titration calorimetry; MD, molecular dynamics.

REFERENCES

- (1) Tejada-Simon, M. V., Zang, Y. C., Hong, J., Rivera, V. M., and Zhang, J. Z. (2003) Cross-reactivity with myelin basic protein and human herpesvirus-6 in multiple sclerosis. *Ann. Neurol.* 53, 189–197.
- (2) Virtanen, J., Wohler, J., Fenton, K., Reich, D., and Jacobson, S. (2014) Oligoclonal bands in multiple sclerosis reactive against two herpesviruses and association with magnetic resonance imaging findings. *Mult. Scler.* 20, 27–34.
- (3) Sullivan, B. M., and Coscoy, L. (2010) The U24 protein from human herpesvirus 6 and 7 affects endocytic recycling. *J. Virol.* 84, 1265–1275.
- (4) Nora-Krukke, Z., Chapenko, S., Logina, I., Millers, A., Platkajis, A., and Murovska, M. (2011) Human herpesvirus 6 and 7 reactivation and disease activity in multiple sclerosis. *Medicina (Kaunas)* 47, 527–531.
- (5) Gustafsson, R., Reitsma, R., Strålfors, A., Lindholm, A., Press, R., and Fogdell-Hahn, A. (2014) Incidence of human herpesvirus 6 in clinical samples from Swedish patients with demyelinating diseases. *J. Microbiol. Immunol. Infect.* 47, 418–421.
- (6) Tait, A. R., and Straus, S. K. (2008) Phosphorylation of U24 from Human Herpes Virus type 6 (HHV-6) and its potential role in mimicking myelin basic protein (MBP) in multiple sclerosis. *FEBS Lett.* 582, 2685–2688.
- (7) Polverini, E., Rangaraj, G., Libich, D. S., Boggs, J. M., and Harauz, G. (2008) Binding of the proline-rich segment of myelin basic protein to SH3 domains: Spectroscopic, microarray, and modeling studies of ligand conformation and effects of posttranslational modifications. *Biochemistry* 47, 267–282.
- (8) Smith, G. S., Homchaudhuri, L., Boggs, J. M., and Harauz, G. (2012) Classic 18.5- and 21.5-kDa Myelin Basic Protein Isoforms Associate with Cytoskeletal and SH3-Domain Proteins in the Immortalized N19-Oligodendroglial Cell Line Stimulated by Phorbol Ester and IGF-1. *Neurochem. Res.* 37, 1277–1295.
- (9) Kramer-Albers, E. M., and White, R. (2011) From axon-glia signalling to myelination: The integrating role of oligodendroglial Fyn kinase. *Cell. Mol. Life Sci.* 68, 2003–2012.
- (10) Biffiger, K., Bartsch, S., Montag, D., Aguzzi, A., Schachner, M., and Bartsch, U. (2000) Severe hypomyelination of the murine CNS in the absence of myelin-associated glycoprotein and fyn tyrosine kinase. *J. Neurosci.* 20, 7430–7437.
- (11) Umemori, H., Sato, S., Yagi, T., Aizawa, S., and Yamamoto, T. (1994) Initial events of myelination involve Fyn tyrosine kinase signalling. *Nature* 367, 572–576.
- (12) Sperber, B. R., Boyle-Walsh, E. A., Engleka, M. J., Gadue, P., Peterson, A. C., Stein, P. L., Scherer, S. S., and McMorris, F. A. (2001) A unique role for Fyn in CNS myelination. *J. Neurosci.* 21, 2039–2047.

- (13) Osterhout, D. J., Wolven, A., Wolf, R. M., Resh, M. D., and Chao, M. V. (1999) Morphological differentiation of oligodendrocytes requires activation of Fyn tyrosine kinase. *J. Cell Biol.* 145, 1209–1218.
- (14) Martin, G. S. (2001) The hunting of the Src. *Nat. Rev. Mol. Cell Biol.* 2, 467–475.
- (15) Smith, G. S., De Avila, M., Paez, P. M., Spreuer, V., Wills, M. K., Jones, N., Boggs, J. M., and Harauz, G. (2012) Proline substitutions and threonine pseudophosphorylation of the SH3 ligand of 18.5-kDa myelin basic protein decrease its affinity for the Fyn-SH3 domain and alter process development and protein localization in oligodendrocytes. *J. Neurosci. Res.* 90, 28–47.
- (16) Harauz, G., and Libich, D. S. (2009) The classic basic protein of myelin: Conserved structural motifs and the dynamic molecular barcode involved in membrane adhesion and protein-protein interactions. *Curr. Protein Pept. Sci.* 10, 196–215.
- (17) Ahmed, M. A., De Avila, M., Polverini, E., Bessonov, K., Bamm, V. V., and Harauz, G. (2012) Solution nuclear magnetic resonance structure and molecular dynamics simulations of a murine 18.5 kDa myelin basic protein segment (S72-S107) in association with dodecylphosphocholine micelles. *Biochemistry* 51, 7475–7487.
- (18) Shelton, H., and Harris, M. (2008) Hepatitis C virus NSSA protein binds the SH3 domain of the Fyn tyrosine kinase with high affinity: Mutagenic analysis of residues within the SH3 domain that contribute to the interaction. *Virol. J.* 5, 24.
- (19) Tait, A. R., and Straus, S. K. (2011) Overexpression and purification of U24 from human herpesvirus type-6 in *E. coli*: Unconventional use of oxidizing environments with a maltose binding protein-hexahistidine dual tag to enhance membrane protein yield. *Microb. Cell Fact.* 10, 51.
- (20) Winterstein, C., Trotter, J., and Kramer-Albers, E. M. (2008) Distinct endocytic recycling of myelin proteins promotes oligodendroglial membrane remodeling. *J. Cell Sci.* 121, 834–842.
- (21) Harris, M., and Coates, K. (1993) Identification of cellular proteins that bind to the human immunodeficiency virus type 1 nef gene product in vitro: A role for myristylation. *J. Gen. Virol.* 74 (Part 8), 1581–1589.
- (22) Cheng, J. T., Hale, J. D., Kindrachuk, J., Jenssen, H., Elliott, M., Hancock, R. E., and Straus, S. K. (2010) Importance of residue 13 and the C-terminus for the structure and activity of the antimicrobial peptide aurein 2.2. *Biophys. J.* 99, 2926–2935.
- (23) Cheng, J. T., Hale, J. D., Elliott, M., Hancock, R. E., and Straus, S. K. (2011) The importance of bacterial membrane composition in the structure and function of aurein 2.2 and selected variants. *Biochim. Biophys. Acta* 1808, 622–633.
- (24) Morton, C. J., Pugh, D. J., Brown, E. L., Kahmann, J. D., Renzoni, D. A., and Campbell, I. D. (1996) Solution structure and peptide binding of the SH3 domain from human Fyn. *Structure* 4, 705–714.
- (25) Edelhoch, H. (1967) Spectroscopic determination of tryptophan and tyrosine in proteins. *Biochemistry* 6, 1948–1954.
- (26) Pace, C. N., Vajdos, F., Fee, L., Grimsley, G., and Gray, T. (1995) How to measure and predict the molar absorption coefficient of a protein. *Protein Sci.* 4, 2411–2423.
- (27) Mal, T. K., Matthews, S. J., Kovacs, H., Campbell, I. D., and Boyd, J. (1998) Some NMR experiments and a structure determination employing a [¹⁵N,²H] enriched protein. *J. Biomol. NMR* 12, 259–276.
- (28) Zarrine-Afsar, A., Mittermaier, A., Kay, L. E., and Davidson, A. R. (2006) Protein stabilization by specific binding of guanidinium to a functional arginine-binding surface on an SH3 domain. *Protein Sci.* 15, 162–170.
- (29) Renzoni, D. A., Pugh, D. J., Siligardi, G., Das, P., Morton, C. J., Rossi, C., Waterfield, M. D., Campbell, I. D., and Ladbury, J. E. (1996) Structural and thermodynamic characterization of the interaction of the SH3 domain from Fyn with the proline-rich binding site on the p85 subunit of PI3-kinase. *Biochemistry* 35, 15646–15653.
- (30) Pettersen, E. F., Goddard, T. D., Huang, C. C., Couch, G. S., Greenblatt, D. M., Meng, E. C., and Ferrin, T. E. (2004) UCSF

Chimera: A visualization system for exploratory research and analysis. *J. Comput. Chem.* 25, 1605–1612.

(31) Yang, Z., Lasker, K., Schneidman-Duhovny, D., Webb, B., Huang, C. C., Pettersen, E. F., Goddard, T. D., Meng, E. C., Sali, A., and Ferrin, T. E. (2012) UCSF Chimera, MODELLER, and IMP: An integrated modeling system. *J. Struct. Biol.* 179, 269–278.

(32) van Gunsteren, W. F., Billeter, S. R., Eising, A. A., Hunenberger, P. H., Krueger, P., Mark, A. E., Scott, W. R. P., and Tironi, I. G. (1996) *Biomolecular simulation: The GROMOS96 manual and user guide*, VdF: Hochschulverlag AG an der ETH Zurich BIOMOS b.v., Zurich.

(33) Scott, W. R. P., Hunenberger, P. H., Tironi, I. G., Mark, A. E., Billeter, S. R., Fennen, J., Torda, A. E., Huber, T., Krueger, P., and van Gunsteren, W. F. (1999) The GROMOS biomolecular simulation program package. *J. Phys. Chem. A* 103, 3596–3607.

(34) Berendsen, H. J. C., Postma, J. P. M., van Gunsteren, W. F., and Hermans, J., (1981) *Intermolecular Forces*, Reidel, Dordrecht, The Netherlands, 331–342.

(35) Berendsen, H. J. C., Postma, J. P. M., van Gunsteren, W. F., Dinola, A., and Haak, J. R. (1984) Molecular-Dynamics with Coupling to an External Bath. *J. Chem. Phys.* 81, 3684–3690.

(36) Ryckaert, J. P., Ciccotti, G., and Berendsen, H. J. C. (1977) Numerical-Integration of Cartesian Equations of Motion of a System with Constraints: Molecular-Dynamics of N-Alkanes. *J. Comput. Phys.* 23, 327–341.

(37) Tironi, I. G., Sperb, R., Smith, P. E., and van Gunsteren, W. F. (1995) A Generalized Reaction Field Method for Molecular-Dynamics Simulations. *J. Chem. Phys.* 102, 5451–5459.

(38) Jia, C. Y., Nie, J., Wu, C., Li, C., and Li, S. S. (2005) Novel Src homology 3 domain-binding motifs identified from proteomic screen of a Pro-rich region. *Mol. Cell. Proteomics* 4, 1155–1166.

(39) Kaneko, T., Kumasaka, T., Ganbe, T., Sato, T., Miyazawa, K., Kitamura, N., and Tanaka, N. (2003) Structural insight into modest binding of a non-PXXP ligand to the signal transducing adaptor molecule-2 Src homology 3 domain. *J. Biol. Chem.* 278, 48162–48168.

(40) Arold, S., O'Brien, R., Franken, P., Strub, M. P., Hoh, F., Dumas, C., and Ladbury, J. E. (1998) RT loop flexibility enhances the specificity of Src family SH3 domains for HIV-1 Nef. *Biochemistry* 37, 14683–14691.

(41) Bochicchio, B., and Tamburro, A. M. (2002) Polyproline II structure in proteins: Identification by chiroptical spectroscopies, stability, and functions. *Chirality* 14, 782–792.

(42) Chellgren, B. W., and Creamer, T. P. (2004) Short sequences of non-proline residues can adopt the polyproline II helical conformation. *Biochemistry* 43, 5864–5869.

(43) Manie, S. N., Astier, A., Haghayeghi, N., Canty, T., Druker, B. J., Hirai, H., and Freedman, A. S. (1997) Regulation of integrin-mediated p130(Cas) tyrosine phosphorylation in human B cells. A role for p59(Fyn) and SHP2. *J. Biol. Chem.* 272, 15636–15641.

(44) Resh, M. D. (1998) Fyn, a Src family tyrosine kinase. *Int. J. Biochem. Cell Biol.* 30, 1159–1162.

(45) Sparks, A. B., Rider, J. E., Hoffman, N. G., Fowlkes, D. M., Quilliam, L. A., and Kay, B. K. (1996) Distinct ligand preferences of Src homology 3 domains from Src, Yes, Abl, Cortactin, p53bp2, PLC γ , Crk, and Grb2. *Proc. Natl. Acad. Sci. U.S.A.* 93, 1540–1544.

(46) Vaynberg, J., Fukuda, T., Chen, K., Vinogradova, O., Velyvis, A., Tu, Y. Z., Ng, L., Wu, C. Y., and Qin, J. (2005) Structure of an ultraweak protein-protein complex and its crucial role in regulation of cell morphology and motility. *Mol. Cell* 17, 513–523.

(47) Kabsch, W., and Sander, C. (1983) Dictionary of protein secondary structure: Pattern recognition of hydrogen-bonded and geometrical features. *Biopolymers* 22, 2577–2637.